HHS Public Access

Author manuscript

Clin Cancer Res. Author manuscript; available in PMC 2017 August 16.

Published in final edited form as:

Clin Cancer Res. 2016 December 15; 22(24): 6278–6289. doi:10.1158/1078-0432.CCR-15-2443.

Image Analysis–based Assessment of PD-L1 and Tumor-Associated Immune Cells Density Supports Distinct Intratumoral Microenvironment Groups in Non–small Cell Lung Carcinoma Patients

Edwin R. Parra[1], **Carmen Behrens**[2], **Jaime Rodriguez-Canales**[1], **Heather Lin**[3], **Barbara Mino**[1], **Jorge Blando**[4], **Jianjun Zhang**[2], **Don L. Gibbons**[2], **John V. Heymach**[2], **Boris Sepesi**[5], **Stephen G. Swisher**[5], **Annikka Weissferdt**[6], **Neda Kalhor**[6], **Julie Izzo**[1], **Humam Kadara**[1], **Cesar Moran**[6], **Jack J. Lee**[3], and **Ignacio I. Wistuba**[1,2]

[1]Departments of Translational Molecular Pathology, The University of Texas MD Anderson Cancer Center, Houston, Texas

[2]Department of Thoracic/Head and Neck Medical Oncology, The University of Texas MD Anderson Cancer Center, Houston, Texas

[3]Department of Biostatistics, The University of Texas MD Anderson Cancer Center, Houston, Texas

[4]Department of Immunology, The University of Texas MD Anderson Cancer Center, Houston, Texas

[5]Department of Thoracic and Cardiovascular Surgery, The University of Texas MD Anderson Cancer Center, Houston, Texas

[6]Department of Pathology, The University of Texas MD Anderson Cancer Center, Houston, Texas

Abstract

Corresponding Author: Ignacio I. Wistuba, Department of Translational Molecular Pathology, Unit 951, The University of Texas MD Anderson Cancer Center, 2130 Holcombe Blvd., Houston, TX 77030. Phone: 713-792-9866; Fax: 713-834-6082; iiwistuba@mdanderson.org.

Note: Supplementary data for this article are available at Clinical Cancer Research Online (http://clincancerres.aacrjournals.org/).

Disclosure of Potential Conflicts of Interest

J.V. Heymach reports receiving commercial research grants from AstraZeneca, Bayer, and GlaxoSmithKline and is a consultant/advisory board member for AstraZeneca, Boerhinger Ingelheim, Eli Lilly, Exelixis, Genentech, GlaxoSmithKline, Novartis, and Synta. N. Kalhor is a consultant/advisory board member for the Bristol-Myers Squibb Immuno-Oncology Pathology Council. No potential conflicts of interest were disclosed by the other authors.

Authors' Contributions

Conception and design: E.R. Parra, J. Rodriguez-Canales, I.I. Wistuba

Development of methodology: E.R. Parra, J. Rodriguez-Canales, B. Mino

Acquisition of data (provided animals, acquired and managed patients, provided facilities, etc.): E.R. Parra, C. Behrens, J.V. Heymach, B. Sepesi, S.G. Swisher, A. Weissferdt, N. Kalhor, C. Moran

Analysis and interpretation of data (e.g., statistical analysis, biostatistics, computational analysis): E.R. Parra, C. Behrens, H.Y. Lin, J. Zhang, J.V. Heymach, S.G. Swisher, H. Kadara, J.J. Lee, I.I. Wistuba

Writing, review, and/or revision of the manuscript: E.R. Parra, H.Y. Lin, J. Blando, J. Zhang, D.L. Gibbons, B. Sepesi, S.G. Swisher, J. Izzo, H. Kadara, J.J. Lee, I.I. Wistuba

Administrative, technical, or material support (i.e., reporting or organizing data, constructing databases): E.R. Parra, J. Rodriguez-Canales, I.I. Wistuba

Study supervision: E.R. Parra

Purpose—We investigated the correlation between immunohistochemical PD-L1 expression and tumor-associated immune cells (TAICs) density in non–small cell lung carcinoma (NSCLC) and correlated them with clinicopathologic variables.

Experimental Design—Tumor tissue specimens from 254 stage I–III NSCLCs [146 adenocarcinomas; 108 squamous cell carcinomas (SCCs)] were examined. PD-L1 expression in malignant cells and macrophages and the density of TAICs expressing CD3, CD4, CD8, CD57, granzyme B, CD45RO, PD-1, FOXP3, and CD68 were evaluated using immunohistochemistry and image analysis.

Results—Malignant cells PD-L1 *H*-score > 5 was detected in 23% of adenocarcinomas and 31% of SCCs, and no significant differences were detected comparing both histologies; the median *H*-score in macrophages was significantly higher in SCC than in adenocarcinoma ($P < 0.001$). In adenocarcinoma, high malignant cells PD-L1 expression and high TAIC density correlated with solid histology, smoking history, and airflow limitation. Multivariate analysis demonstrated that high CD57-positive cell density correlated with better recurrence-free survival (RFS; $P = 0.0236$; HR, 0.457) and overall survival (OS; $P = 0.0261$; HR, 0.481) rates for SCC. High CD68-positive cell density in intratumoral compartment correlated with better RFS ($P = 0.0436$; HR, 0.553) for adenocarcinoma. The combination of low CD4/CD8/C68-positive cell density and PD-L1 *H*-score >5 in malignant cells identified small subset of adenocarcinomas with worse outcomes (RFS: $P = 0.036$; HR, 4.299; OS: $P = 0.00034$; HR, 5.632).

Conclusions—We detected different PD-L1 expression and TAIC density patterns in NSCLC. Distinct groups of tumor microenvironment correlated with NSCLC clinicopathologic features, including outcome.

Introduction

Multiple genetic and epigenetic changes in patients with several cancer types cause resistance to immune attack of tumors by inducing specific T-cell tolerance against tumor and expression of ligands that engage inhibitory receptors and block T-cell activation, resulting in T-cell anergy or exhaustion in the tumor microenvironment (1). In this process, programmed cell death protein 1 (PD-1), a T-cell co-inhibitory receptor, and one of the protein's ligands, programmed cell death ligand 1 (PD-L1; B7-H1 or CD274), play pivotal roles in the ability of tumor cells to evade the host's immune system. Although virtually absent from normal cells except macrophages, PD-L1 expression can be induced in a variety of cell types, including antigen-presenting, B, T, epithelial, muscle, and vascular endothelial cells and trophoblasts (2). The physiologic role of PD-L1 is to bind to PD-1 receptors expressed on the surface of activated cytotoxic T cells (2). This binding causes inhibition of IL2 production and T-cell activation via reduced phosphorylation of ζ-chain–associated protein kinase 70 and protein kinase C θ (3). PD-1/PD-L1 interaction serves as an important regulatory checkpoint for excessive adaptive immune responses to antigens and autoimmunity. Researchers have observed and evaluated PD-L1 expression in malignant cells of a number of tumor types, including melanoma and breast, colorectal, and lung cancers (4–11).

Therapies blocking the PD1/PD-L1 axis have resulted in different rates of tumor response for a variety of cancer types (12). For example, antibody-mediated blockade of PD-L1 induced durable tumor regression and prolonged disease stabilization in patients with a variety of solid tumors, including non–small cell lung carcinoma (NSCLC; refs. 12, 13). Although these studies demonstrated correlation between immunohistochemical (IHC) PDL1 expression in NSCLC cells and clinical responses to anti-PD-1 and anti-PD-L1 antibodies (12, 13), some patients with tumors negative for PD-L1 expression had responses to similar to those in patients with tumors positive for PD-L1 expression (14). Recently, investigators showed that across several cancer types, including NSCLC, patients with tumors expressing PD-L1 at high levels in both malignant cells and tumor-associated immune cells (TAIC) had responses to anti-PD-L1 therapy (11). Taken together, these findings suggested that factors other than PD-L1 in the tumor microenvironment, including tumor-infiltrating lymphocytes (TIL; refs. 15, 16) and tumor-associated macrophages (TAM; ref. 17), may drive responses to anti-PD-1 and anti–PD-L1 therapies and be involved in lung cancer pathogenesis and progression (10, 11, 18).

Researchers in a number of studies have characterized PD-L1 protein expression in surgically resected stage I–IV NSCLC tumors using IHC or immunofluorescence (7, 8, 11, 15, 16) with formalin-fixed, paraffin-embedded tumor specimens and correlated the findings with outcome. Although most of the studies demonstrated that high PD-L1 protein expression correlated with better outcome than did low expression (8, 11, 18, 19), some authors reported no association of PD-L1 expression with outcome (9, 15) or that the expression correlated with poor prognosis (10). Most of these studies differed in the type of specimens used [whole histologic sections vs. tissue microarrays (TMA)], type of protein expression analysis (IHC vs. immunofluorescence), and quantification assessment (image analysis vs. microscopic observation; refs. 7–11, 15–19). Researchers in only a few studies have attempted to correlate the expression of PD-L1 with TAIC density and characteristics, particularly TILs, using a limited number of IHC markers (e.g., CD8, CD45RO; refs. 15, 19) or simple histologic evaluation (7, 11). To date, no published studies have included assessment of a comprehensive panel of immune markers in NSCLC cases using image analysis to characterize the association among PD-L1 expression, immune cell response, and clinicopathologic features of tumors to determine distinct subgroups of NSCLC and patients' outcome. Therefore, in the present study, we characterized the IHC expression of a large panel of immune markers PD-L1, PD-1, and 8 others and assessed the TAIC density in both the peritumoral and intratumoral compartments in surgically resected NSCLC specimens. To assess this objectively, we performed quantitative image analysis and correlated the findings with the patients' clinical features and their tumors' pathologic and molecular features.

Materials and Methods

Cases and specimens

Formalin-fixed, paraffin-embedded histological sections of surgically resected primary NSCLC tumors obtained from 254 patients who underwent surgery with curative intent from 1997 to 2012 at The University of Texas MD Anderson Cancer Center (Houston, TX) were

used. The study patients had either adenocarcinoma (n=146) or squamous cells carcinoma (SCC; n=108) and did not receive neoadjuvant therapy. Tumor staging was performed using the staging system from the 7th American Joint Committee on Cancer (AJCC; ref. 20). For adenocarcinoma, predominant histologic pattern (solid, lepidic, acinar, papillary, and micropapillary) was determined according to the 2015 World Health Organization classification (21). For SCC grading, we used well, moderate, and poorly differentiated categories. In a subset of cases (n = 130; 97 adenocarcinomas and 33 SCCs), PD-L1 IHC expression was assessed in paired whole tissue sections and TMA samples. Of these, all 3 TMA cores were available in 73 adenocarcinoma and 24 SCCs, whereas the rest of the cases had 2 cores available for analysis. The TMA sections were prepared using three 1.0-mm tissue cores obtained from the center, middle, and periphery of the tumor, as described previously (22). Data on nonreversible airflow limitation, defined as a ratio of the forced expiratory volume in 1 second to the forced vital capacity of less than 0.7 (23), were available for a large subset of our patients (n= 179). *EGFR* and *KRAS* mutation data obtained using Sanger sequencing were available in 91% (n=137) of adenocarcinomas. This study was approved by the MD Anderson Institutional Review Board.

IHC staining

Four-micrometer-thick sequential histologic tumor sections were obtained from a representative formalin-fixed, paraffin-embedded tumor block and used for IHC analysis. IHC was performed using an automated staining system (BOND-MAX; Leica Microsystems) with antibodies against PD-L1 (clone E1L3N, dilution 1:100; Cell Signaling Technology), CD3 (T-cell lymphocytes; dilution 1:100; Dako), CD4 (helper T cell; Novocastra; clone 4B12, dilution 1:80; Leica Biosystems), CD8 (cytotoxic T cell; clone CD8/144B, dilution 1:20; Thermo Fisher Scientific), CD57 (natural killer T cell; clone HNK-1, dilution 1:40; BD Biosciences), granzyme B (cytotoxic lymphocytes; clone F1, ready to use; Leica Biosystems), CD45RO (memory T cell; clone UCHL1, ready to use; Leica Biosystems), PD-1 (clone EPR4877-2, dilution 1:250; Abcam), FOXP3 (regulatory T cell; clone 206D, dilution 1:50; BioLegend), and CD68 (macrophages; clone PG-M1, dilution 1:450; Dako). Expression of all of the markers in cells was detected using a Novocastra Bond Polymer Refine Detection kit (Leica Microsystems) with a diaminobenzidine reaction to detect antibody labeling and hematoxylin counterstaining. Positive and negative controls were used for PD-L1 IHC expression (human embryonic kidney 293 cell line transfected and nontransfected with PD-L1 gene and human placenta and tonsil FFPE tissues) during each run IHC staining using autostainers. For the TAIC IHC expression, human tonsil FFPE tissues with and without primary antibody were used as positive and negative controls, respectively, with each run IHC staining.

Image analysis

To measure the IHC expression of the different markers and quantify the inflammatory cells expressing the slides, containing whole-tumor sections or immunohistochemically stained TMA sections, were digitally scanned at ×200 magnification using a ScanScope Aperio AT Turbo slide scanner (Leica Microsystems). The images were visualized using the ImageScope software program (Leica Microsystems) and analyzed using the Aperio Image Toolbox and GENIE image analysis tool (Leica Microsystems). The pathologist who

performed the image analysis was blinded to patients' outcome. After training, the software by a pathologist (Supplementary Fig. S1), membranous PD-L1 expression in malignant epithelial cells and macrophages was analyzed using a cell membrane staining algorithm, and the staining intensity scored as 0 (no staining), 1+ (weak staining), 2+ (moderate staining), or 3+ (strong staining) and extension (percentage) of expression were determined (Fig. 1). The PD-L1 *H*-scores for tumor tissues were determined by multiplying the staining intensity and reactivity extension values (range, 0–300). The densities of cells expressing CD3, CD4, CD8, CD57, granzyme B, CD45RO, PD-1, and FOXP3 were evaluated using the Aperio nuclear algorithm and CD68 using Aperio cytoplasmic algorithm (Fig. 2 and Supplementary Fig. S2) and counting the cells positive for them in 5 random square areas (1 mm^2 each) in both intratumoral and peritumoral compartments. While 5 intratumoral regions were available in all cases and 24 tumors did not have peritumoral regions for analysis. Histologic assessment of each 1 mm^2 was performed to ensure that tumor tissue (at least 80% malignant cells and tumor stroma) was included in the selected intratumoral region, and only non-malignant cells were included in the peritumoral compartment. For this analysis, each area examined was overlapped with the sequential IHC slides to quantify each marker at the same location of the tumor specimens. The average total number of cells positive for each marker in the 5 square areas was expressed in density per mm^2. Similar to PD-L1 *H*-score from 5 intratumoral areas, the TMA was scored as the median PD-L1 *H*-score average of all cores from each case. In addition, as has been proposed by Teng and colleagues (24), 4 different types tumor microenvironment we were able to identify based on the density of TILs and the expression of PD-L1, as follows: type I (adaptive immune resistance), type II (immunologic ignorance), type III (intrinsic induction), and type IV (tolerance). Combining PD-L1 expression in malignant cells (>5% was considered positive) with the density of cells expressing CD3 using 3 levels (tertile) divided on the basis of regular values of distribution by the statistical software (moderate and severe density were considered positive), we were able to identify the frequency of those four subtypes of tumor' microenvironment in our NSCLC cases.

PD-L1 mRNA analysis

Total RNA extracted from the NSCLC specimens with fresh-frozen tissue available was used to measure PD-L1 gene expression using an available probe with a human WG-6 v.3 Expression BeadChip (Illumina). Resulting data set for 104 primary adenocarcinomas and 39 primary SCCs (SPORE dataset; GSE41271) were deposited in the Gene Expression Omnibus repository (25).

Statistical methods

The χ^2 test or Fisher exact test was used to examine differences in categorical variables, and the Wilcoxon rank-sum test and Kruskal–Wallis test were used to detect differences in continuous variables between groups of patients. The recurrence-free survival (RFS) and overall survival (OS) distributions for the patients were estimated using the Kaplan–Meier method. RFS was defined as the interval from surgery to recurrence or last contact, and OS was defined as the interval from surgery to death or last contact. Both RFS and OS data were censored at 5 years if a patient was alive or died beyond 5 years. A log-rank test was performed to determine the difference in survival between the groups. Regression analysis of

the RFS and OS data was performed using Cox proportional hazards model. The statistical software programs SAS (version 9.2; SAS Institute, Inc.) and S-Plus (version 8.04; TIBCO) were used to perform the computations for all analyses.

Results

PD-L1 protein expression

Clinicopathologic and molecular data on the patients are shown in Table 1. Our image analysis–based examination of whole tumor sections obtained from the 146 patients with adenocarcinoma and 108 patients with SCC demonstrated that the median PD-L1 H-score in malignant cells was low for both tumor histologies (median, 1.29 for adenocarcinoma vs. 0.95 for SCC). We found no significant differences in PD-L1 *H*-score between the 2 histologies ($P = 0.326$; Fig. 1).

In addition, we determined the distribution of lung tumors using 5 cutoff percentages of malignant cells with PD-L1 expression according to histology: >1%, 87 adenocarcinomas (60%) and 52 SCCs (48%); >5%, 34 adenocarcinomas (23%) and 34 SCCs (31%); >10%, 31 adenocarcinomas (21%) and 29 SCCs (27%); >20%, 21 adenocarcinomas (14%) and 25 SCCs (23%); and >50%, 9 adenocarcinomas (6%) and 12 SCCs (11%). Whereas SCC specimens exhibited higher PD-L1 expression than did adenocarcinoma specimens at all cutoff percentages examined, the difference was statistically significant at only greater than 5% ($P=0.003$), greater than 10% ($P < 0.0001$), and greater than 20% ($P = 0.020$).

PD-L1 expression in cells with characteristics of TAMs was higher than that in malignant cells for both tumor histologies, whereas SCC specimens exhibited significantly higher PD-L1 *H*-scores in macrophages than did adenocarcinoma specimens (median, 39.89 and 18.08, respectively; $P < 0.001$).

Comparison of IHC PD-L1 expression in whole histologic tumor sections and TMA sections

To compare IHC PD-L1 expression levels in whole histologic tumor sections and TMA sections, we looked at the *H*-scores for malignant cells only and for malignant cells and TAMs together in a subset of adenocarcinoma ($n = 97$) and SCC ($n = 33$) specimens. In our analysis of malignant cells only, we found that PD-L1 expression in whole histologic sections correlated positively and significantly with that in TMA sections for both histologies (adenocarcinoma: $r = 0.417$, $P < 0.0001$; SCC: $r = 0.438$, $P = 0.0108$). In addition, in our analysis of malignant cells and TAICs in 5 randomly selected 1-mm^2 areas of tumor specimens, we again found that PD-L1 expression in whole histologic sections correlated positively and significantly with that in TMA sections (adenocarcinoma: $r = 0.617$, $P < 0.0001$; SCC: $r = 0.502$, $P = 0.003$). Taken together, these data suggested that the 3 TMA cores were good surrogates for whole tumor sections in PD-L1 expression analysis of NSCLC. In addition, we observed a positive and significant correlation between the expression of PD-L1 in malignant cells and TAMs in whole histologic tumor sections and that in the five 1-mm^2 areas of the specimens (adenocarcinoma: $r = 0.575$, $P < 0.0001$; SCC: $r = 0.733$, $P < 0.0001$).

Correlation between PD-L1 protein and PD-L1 gene expression

To assess the correlation between PD-L1 protein and PD-L1 gene expression in NSCLC cases, we studied 104 adenocarcinoma and 39 SCC specimens with available data on PD-L1 mRNA expression. We found that PD-L1 mRNA expression in whole tumor specimens correlated positively and significantly with PDL1 protein expression for both NSCLC histologies when we assessed the PD-L1 protein expression in the entire population of tumor cells, including both malignant cells and TAMs, in 5 random areas of the whole tumor specimens (adenocarcinoma: $r = 0.448$, $P < 0.0001$; SCC: $r = 0.634$, $P < 0.0001$) and TMA sections (adenocarcinoma: $r = 0.443$, $P < 0.0001$; SCC: $r = 0.428$, $P = 0.02$). Similarly, we found positive and significant correlations of PD-L1 gene and protein expression when we examined protein expression in malignant cells only in whole histologic tumor sections (adenocarcinoma: r=0.323, P=0.0008; SCC: r= 0.398, $P = 0.012$). These data indicated that PD-L1 mRNA expression is a good potential surrogate for PD-L1 protein expression in whole NSCLC tumor tissue.

Correlation between PD-L1 expression and clinicopathologic features of NSCLC

In adenocarcinoma specimens, the PD-L1 *H*-score greater than the median in malignant cells correlated with smoking history, airflow limitation, and tumor differentiation. The PD-L1 *H*-score was significantly higher in ever-smokers (mean, 11.41; median, 1.45, $P < 0.0001$) than in never-smokers (mean, 1.31; median, 0.56, $P < 0.0001$). In comparison, the PD-L1 *H*-score in adults who have smoked at least 100 cigarettes in their lifetime and quit smoking at least a year before surgery, former smokers (mean, 10.24; median, 1.43) did not differ significantly from that in current smokers (mean, 12.82; median, 1.64; $P = 0.918$). Also, patients with adenocarcinoma with irreversible airflow limitation (forced expiratory volume in 1 second/forced vital capacity ratio < 0.7) had a significantly higher PD-L1 *H*-score in malignant cells in whole tumor specimens (median, 1.44 versus 1.11; $P = 0.048$) and 5 random areas of the tumor specimens (median, 30.78 vs. 15.98; $P = 0.014$) than did patients without airflow limitation (Supplementary Table S1). Adenocarcinoma specimens with a solid tumor histologic pattern had significantly higher PD-L1 *H*-scores in malignant cells ($P = 0.021$; average, 15.46; median, 1.69) than did specimens with a non-solid tumor histologic pattern (mean, 3.57; median, 1.13). In addition, as we detected at the protein level, we found that PD-L1 gene expression was significantly higher in adenocarcinoma specimens with a solid tumor histology than in those with a non-solid tumor histology ($P < 0.0001$). PD-L1 expression in malignant cells was lower in *EGFR*-mutant adenocarcinoma specimens (mean *H*-score, 5.97; median *H*-score, 1.39) than in adenocarcinoma specimens wild-type for *EGFR* (mean H-score, 9.65; median *H*-score, 1.07), but the difference was not significant ($P = 0.071$). We did not detect an association between PD-L1 expression and *KRAS* mutation in adenocarcinoma specimens. We observed no other correlations between PD-L1 expression and other clinical and pathologic features for either histological type of NSCLC.

TAIC density

Our image analysis–based IHC examination of TAICs included that of immune markers identifying TILs ($CD3^+$), helper T cells ($CD4^+$), cytotoxic T cells ($CD8^+$ or granzyme B^+), natural killer T cells ($CD57^+$), memory T cells ($CD45RO^+$), regulatory T cells ($PD\text{-}1^+$ or

FOXP3$^+$), and TAMs (CD68$^+$) in 5 randomly selected 1-mm^2 areas of tumor specimens. Representative images of immunohistochemical stains of TAICs for these markers are shown in Fig. 2. We found that both adenocarcinoma and SCC specimens had various TIL densities, particularly when we examined the intratumoral and peritumoral compartments separately (Table 2; Supplementary Table S2). Unexpectedly, we found in both tumor types and compartments examined that the number of CD4$^+$CD8$^+$ cells was slightly larger than the number of CD3$^+$ cells and that the number of cells expressing granzyme B was significantly lower than cells expressing CD8. In the peritumoral compartment, SCCs exhibited higher density of cells expressing all markers except PD-1 in TILs, with statistically significantly higher levels of cells expressing CD3 ($P = 0.0010$), CD8 ($P = 0.0020$), granzyme B ($P = 0.0490$), CD45 ($P < 0.0001$), and FOXP3 ($P = 0.0010$) than that in adenocarcinomas. In the intratumoral compartment, the differences in TAICs density between the 2 tumor histologies were less noticeable. We did observe that adenocarcinoma specimens had significantly higher densities of CD3$^+$ ($P = 0.0030$), CD4$^+$ ($P < 0.0001$), and CD57$^+$ ($P < 0.0001$) cells than SCC specimens' did. Similar to TILs, the density of cells expressing CD68 was significantly higher in the peritumoral compartment than in intratumoral areas for both tumor histologies ($P < 0.0001$) and significantly higher in the intratumoral region in adenocarcinoma than in SCC specimens ($P < 0.0001$). These findings indicated that the densities of TILs and TAMs vary according to the tumor compartment and NSCLC histology.

PD-L1 expression and TAIC density

When we examined the correlation of PD-L1 *H*-score in malignant cells with TIL and TAM densities in whole-tumor histologic sections, we found different patterns of correlation according to NSCLC histology and tumor compartment. In adenocarcinoma specimens, density of cells expressing the majority of TAIC markers examined exhibited a positive significant correlation with expression of PD-L1 in malignant cells in the intratumoral (7 of 9 comparisons) and peritumoral (8 of 9 comparisons) compartments (Supplementary Table S3). The cells expressing markers whose level was not significantly correlated with PD-L1 expression in adenocarcinomas were positive for CD68 in both compartments and CD45RO in the intratumoral region. In SCC specimens, we found lower correlation of PD-L1 expression with TAIC markers' expression, with 4 of 9 markers (CD3, CD8, granzyme B, and CD45RO) significantly and positively correlated with PD-L1 expression in the intratumoral area and one marker (CD3) significantly and positively correlated with PD-L1 expression in the peritumoral region (Supplementary Table S3). The PD-L1 *H*-score in TAMs exhibited a lower rate of correlation with marker expression in TAICs for both NSCLC histologies and in both tumor compartments than did the PD-L1 expression in malignant cells (Supplementary Table S4).

Combining PD-L1 expression in malignant cells with the density of cells expressing CD3 as proposed by Teng and colleges (24), we were able to identify the 4 subtypes of tumor microenvironment in our NSCLC cases as shown in Table 3. This analysis showed that 29% in adenocarcinoma and 26% in SCC had an immune ignorance phenotype and that pattern most frequently observed (adenocarcinoma 48% and SCC 43%) was tumors with immune tolerance pattern defined as positive TILs without PD-L1 expression in malignant cells.

Cases with positive PD-L1 expression and positive TILs defined as tumors with adaptive immune resistance pattern were found in 19% of adenocarcinoma and 31% of SCC. Tumors with the intrinsic induction patters were less frequently detected (adenocarcinoma 3% and SCC 7%). Similar percentages of cases in each group were found when the analysis included $CD4^+$ and $CD8^+$ TILs, as well as $CD3^+$ and $CD68^+$ TAICs (data not shown).

Correlation between TAIC density and clinicopathologic features of NSCLC

TAIC density correlated with clinical and pathologic tumor features only in adenocarcinoma specimens. Specifically, these specimens with any solid tumor histology had significantly higher levels of TILs in the intratumoral (cells expressing CD3, CD8, granzyme B, and PD-1) and peritumoral (cells expressing CD3, CD4, CD8, granzyme B, CD45RO, PD-1, and FOXP3) compartments than did adenocarcinoma specimens with non-solid tumor histologies (Supplementary Table S5). Tumor specimens obtained from ever-smokers had significantly higher granzyme B expression in both compartments and higher peritumoral CD8 expression than did those obtained from never-smokers, whereas tumor specimens obtained from never-smokers had higher intratumoral CD4 expression. Overall, tumor specimens obtained from current smokers had a significantly higher TAIC density (cells positive for CD3, CD8, CD57, granzyme B, PD-1, and FOXP3), mostly in the peritumoral compartment than did those obtained from former smokers and never-smokers (Supplementary Table S5). Patients with airflow limitation had overall higher numbers of TAICs in both compartments than did patients without airflow limitation (Supplementary Table S1). Furthermore, we observed significantly higher TILs expressing granzyme B and FOXP3 in the intratumoral compartment and cells expressing CD3, CD4, CD8, granzyme B, and CD45RO in the peritumoral compartment in tumors from patients with airflow limitation (Supplementary Table S2). Tumors larger in diameter than the median (3.1 cm) exhibited greater overall TAIC densities in the peritumoral region (cells expressing CD3, CD8, granzyme B, PD-1, or FOXP3) than in the intratumoral region (CD4), whereas smaller tumors had higher densities of CD4-positive cells in the intratumoral compartment than in the peritumoral one. Of note, adenocarcinoma specimens with *EGFR* mutations had more intratumoral cells expressing CD57 and CD45RO and peritumoral cells expressing CD3 and CD4 than did specimens wild-type for *EGFR*. We did not detect a correlation between TAIC density and *KRAS* mutation in adenocarcinoma specimens.

Correlation between immune markers expression and NSCLC prognosis

PD-L1 expression *H*-score and percentage of expression at various cutoff levels in malignant cells was not significantly correlated with the outcome of NSCLC in our multivariate analysis. However, in adenocarcinoma specimens, our univariate analysis demonstrated that PD-L1 *H*-scores higher than the median [$P = 0.070$; HR, 1.746; 95% confidence interval (CI), 0.955–3.190]] and greater than 5 ($P = 0.051$; HR, 1.128; 95% CI, 1.000–1.274) were nonsignificantly correlated with a poor OS duration (Fig. 3A). In SCC specimens, PD-L1 *H*-scores higher than the median in macrophages correlated significantly with poor OS durations ($P = 0.036$; HR, 0.548; 95% CI, 0.312–0.961) and indicated a nonsignificant trend of poor RFS durations ($P=0.063$; HR, 0.565; 95% CI, 0.309– 1.033) in our univariate analysis (Fig. 3B).

In addition, the density of TAICs expressing several immune markers in tumor specimens correlated with NSCLC outcome in univariate and multivariate analyses. For the patients with adenocarcinoma, intratumoral densities of cells expressing CD4 and FOXP3 greater than the median density were significantly correlated with good RFS and OS durations, respectively, in univariate analysis (data not shown). For the patients with SCC, peritumoral densities of cells expressing CD57 greater than the median density were significantly associated with good RFS and OS durations, respectively, in both univariate (data not shown) and multivariate (RFS: $P = 0.0236$; HR, 0.457; 95% CI, 00.232–0.900; OS: $P = 0.0261$; HR, 0.481; 95% CI, 0.258–0.91]) analyses after adjustment for tumor stage and adjuvant therapy (Fig. 3C and D). In addition, our multivariate analysis demonstrated that intratumoral CD68-positive cell densities greater than the median correlated with good RFS durations for patients with adenocarcinoma ($P = 0.0436$; HR, 0.553; 95% CI, 0.311–0.983; Fig. 3E) and a nonsignificant trend of correlation with poor RFS durations for patients with SCC (P=0.0811; HR, 1.751; 95% CI, 0.033–3.287). Furthermore, the combination of CD4/CD8/C68-positive cell densities lower than the median and PD-L1 *H*-scores greater than 5 in malignant cells identified a small subset of patients with adenocarcinoma with poor outcomes (RFS: P=0.036; HR, 4.299; 95% CI, 1.415–13.059; OS: $P = 0.00034$; HR, 5.632; 95% CI, 2.015–15.737; Fig. 3F).

Discussion

In this study, we examined archived tumor specimens obtained from a large cohort of patients with stage I–III NSCLC, both adenocarcinoma ($n = 146$) and SCC ($n = 108$), for IHC expression of PD-L1 in malignant cells and macrophages and density of TAICs (TILs and TAMs) expressing CD3, CD4, CD8, CD57, granzyme B, CD45RO, PD-1, FOXP3, and CD68 in intratumoral and peritumoral compartments using image analysis. We detected PD-L1 *H*-scores > 5 in malignant cells in 23% of the adenocarcinoma specimens and 31% of the SCC specimens and found that the median *H*-score in macrophages was markedly higher in SCC specimens than in adenocarcinoma specimens. In adenocarcinoma specimens, high PD-L1 expression in malignant cells and high TAIC densities correlated with solid tumor histology, airflow limitation, and smoking history. For TAICs expressing most of the immune markers tested, the cell density was significantly higher in peritumoral than in intratumoral compartments for both tumor histologies, and SCC s exhibited higher peritumoral densities than did adenocarcinomas. Multivariate analysis of outcome demonstrated that the combination of low CD4/CD8/C68-positive cell density and high PD-L1 expression in malignant cells identified a small subset of patients with adenocarcinoma with poor RFS and OS durations. We concluded that the PD-L1 protein expression pattern and TAIC density differ in surgically resected adenocarcinoma and SCC specimens and that TAIC density varies according to tumor compartment. Importantly, in the present study, we identified distinct tumor environment patterns in NSCLC, and several immune markers whose expression correlated with outcome of surgical resection tumors.

As described previously (7, 8, 15, 16, 19), we observed relatively low levels of expression of PD-L1 in malignant cells in NSCLC specimens. In particular, SCCs had slightly higher levels of PD-L1 expression in malignant cells than did adenocarcinomas, particularly for cutoff percentages greater than 5%, 10%, and 20%. The clinically relevant threshold for IHC

PD-L1 expression in NSCLC cells has yet to be defined, and researchers have examined various cutoffs of PD-L1 positivity, including at least 5%(7, 9, 26),10%(15), and50%(8, 16) cells and greater than the median *H*-score (10, 27). The cutoff most frequently used to assess IHC PD-L1 expression in malignant cells in patients with NSCLC given PD-1/PD-L1 inhibitors has been at least 5% cells, and this cutoff value has been associated with durable tumor regression and prolonged disease stabilization in response to anti-PD-L1 treatment in advanced metastatic NSCLC cases (14). In the present study, 23% of the adenocarcinoma specimens and 31% of the SCC specimens had more than 5% of malignant cells with PD-L1 expression, which was not markedly different from the percentages reported by others (7, 27). In addition, we found high levels of PD-L1 expression in cells with characteristics of macrophages for both NSCLC histologies, with markedly higher expression in SCC than in adenocarcinoma specimens. To the best of our knowledge, we are the first to specifically analyze and quantify TAMs expressing PD-L1 in NSCLC specimens using IHC. PD-L1 expression in macrophages is biologically relevant and may be associated with tumor progression. As shown in a study using an experimental inflammatory macrophages mouse model (28), PDL1 expression was induced in macrophages using the same cytokines, such as IFNγ and VEGF, involved in the PD-L1 upregulation of human cancer cell lines (29), leading to effective suppression of T-cell immunity.

Comparison of different reports of PD-L1 expression in NSCLC cases in the literature is hindered by the use of several analytical methodologies. In most studies, investigators undertook PD-L1 analysis using whole-tissue sections (7, 9, 10, 16, 19, 26, 27) and some studied TMAs (8, 11, 15). Examination of whole-tissue sections may lead to more frequent identification of PD-L1–positive cases than that using more limited sampling with a TMA. However, the present study surprisingly demonstrated that PD-L1 expression in malignant cells in whole-tumor sections correlated markedly and positively with the expression in TMA sections for both NSCLC types. In addition, the data on whole tumor sections correlated with that obtained via examination of 5 randomly selected 1-mm^2 areas of tumor specimens. Taken together, these data demonstrated for the first time that TMA sections and randomly selected areas of tumor specimens are reliable surrogates for whole-tumor sections in sampling approaches to assessing PD-L1 expression in patients with NSCLC.

We examined PD-L1 in malignant cells and macrophages and TAICs density using a quantitative computer-based image analysis system. In most of the previously reported studies of NSCLC, researchers used semiquantitative PD-L1 and TAIC density scoring systems on the basis of microscopic observation of slides by a trained pathologist (7–10, 15, 16, 19, 26, 27). Visual evaluation of immunohistochemically stained tissue sections remains a rather subjective process characterized by significant intraobserver and interobserver variability and reduced reproducibility, which digital image analysis can overcome (30, 31).

The PD-L1 *H*-score in malignant cells correlated with smoking history and airflow limitation in patients with adenocarcinoma. The *H*-score was markedly higher in ever-smokers than in never-smokers, but we detected no difference between former and current smokers. In addition, we found markedly higher PD-L1 expression in malignant cells in patients with airflow limitation, a condition closely associated with chronic obstructive

pulmonary disease (23), than in patients without it, suggesting a link between inflammatory processes affecting the lungs of smokers and immune response statuses of tumors.

In our study, specimens of both NSCLC histologies had higher numbers of TAICs in the peritumoral compartment than in the intratumoral region. Also, we found distinct TIL and TAM infiltration patterns in specimens of both histologies when we examined both compartments, with SCC specimens exhibiting higher numbers of TILs expressing immune markers (except PD-1) than those in adenocarcinoma specimens in the peritumoral compartment. We hypothesized that nonhomogeneous or clustered secretion of cytokines and chemokines at the invasive tumor margin may enhance the recruitment of different TAIC subtypes to the tumor microenvironment (32). Interestingly, PD-L1 expression in malignant cells was markedly correlated with the TAIC density in both tumor compartments for both NSCLC histologies. These observations are supported by previous findings that different immune cells, such as $CD8^+$ and $CD4^+$ cells and natural killer cells, are capable of inducing PD-L1 expression in malignant cells via IFNγ production (33). Curiously, although we found a significant correlation between PD-L1 IHC expression in malignant cells and infiltration of $PD\text{-}1^+$ cells in adenocarcinoma, this was not observed in SCC suggesting different microenvironment mechanism(s) of immune resistance between these 2 NSCLC histology types. In our study, we characterized the 4 types of tumor microenvironment described by Teng and colleagues (24) using as criteria for TIL density levels of $CD3^+$ cells combined with PD-L1 expression in malignant cells. We found that most tumors demonstrate an immune tolerance phenotype defined as positive TILs without PD-L1 expression and tumors with intrinsic induction pattern defined as positive PD-L1 expression and lack of TILs are rarely observed in surgically resected NSCLCs.

Our TAICs quantitative image analysis of NSCLC encountered a couple of unexpected findings. The number of $CD4^+CD8^+$ cells was slightly larger than the number of $CD3^+$ cells in both tumor types and compartments examined. Potential explanations to this finding include that CD4 is expressed in various immune cells such as monocytes/macrophages, eosinophils, $CD34^+$ progenitor cells, and natural killer cells (34) and that double $CD4/CD8^+$ T cells have been described in several pathological conditions as well as in normal individuals (35). Also, we found that the number of cells expressing granzyme B was significantly lower than the cells expressing CD8. Interestingly, it has been reported that a decreased proportion of granzyme B^+ cells in lung tumors was a result of soluble mediators, not identified yet, secreted probably by cancer cells (36).

In addition, we observed that TAIC density correlated with clinical and pathologic tumor features only in adenocarcinoma specimens. In these specimens, the presence of any solid tumor histology, smoking history, and airflow limitation was correlated with higher overall numbers of TILs in intratumoral and peritumoral compartments than was a non-solid tumor histology. Smoking status and pulmonary disorders with airflow limitation such as chronic obstructive pulmonary disease are associated with greater risk of lung cancer than patients without those characteristics and are characterized by abundant and deregulated inflammation (37). The selective recruitment of TILs ($CD3^+$), helper T cells ($CD4^+$), cytotoxic T cells ($CD8^+$ and granzyme B^+), and memory T cells ($CD45RO^+$), to the peritumoral compartment of these lung tumors suggests that these TAICs, which are located

around the tumors, are less affected by tumor-derived inhibitory factors than are cells located in direct contact with malignant cells in the intratumoral compartment.

Although the present study did not demonstrate that PD-L1 expression in malignant cells is an independent prognostic factor for NSCLC, our univariate analysis demonstrated a nonsignificant trend of correlation of a PD-L1 *H*-score greater than 5 in adenocarcinoma specimens with poor OS duration as reported previously (15, 26). Notably, we report herein for the first time that a PD-L1 *H*-score higher than the median in macrophages correlated significantly with poor OS duration and demonstrated a nonsignificant trend of poor RFS rate in patients with SCC in univariate analysis. Accumulating studies have demonstrated that increased TAM density is associated with poor prognosis for NSCLC (38, 39), suggesting that macrophages are targets for therapy for this cancer. Recently, a study showed that a fraction of macrophages in peritumoral stroma from patients with hepatocellular carcinoma expressed PD-L1 and was attenuated by blocking PD-L1 activity in these cells; the accumulation of these macrophages in the peritumoral stroma also predicted poor prognostic survival in these patients (40).

Increased TIL numbers have been associated with increased survival durations for both early-stage and advanced NSCLC (11, 41, 42). In the present study, the TAIC density correlated with NSCLC outcome in univariate and multivariate analyses. The presence of increased numbers of cells expressing intratumoral CD4 or FOXP3 and macrophages in adenocarcinoma specimens and of increased numbers of cells expressing intratumoral and peritumoral CD57 in SCC specimens were associated with OS or RFS. Only the numbers of cells expressing CD4, CD57, or FOXP3 independently indicated better prognosis in patients with adenocarcinoma in multivariate analysis, although. However, studies using IHC analysis of TILs in surgically resected NSCLC specimens have had conflicting results. One study demonstrated an association between increased numbers of cytotoxic ($CD8^+$) but not helper T ($CD4^+$) cells with increased survival duration (43), whereas others had opposite results or did not demonstrate a survival benefit (44, 45). Similar to our findings, increased natural killer cell ($CD57^+$) infiltration in several types of tumors has been associated with good clinical outcome (46, 47), including for lung SCC (48).

A key understudied issue in lung cancer is the potential for TAIC density to predict response to immunostimulatory therapies and patient outcomes. Studying 3 important immune cell populations helper T cells ($CD4^+$), cytotoxic T cells ($CD8^+$), and macrophages ($CD68^+$; ref. 49), we found that the combination of low CD4/CD8/CD68-positive intratumoral density and high PD-L1 expression in malignant cells identified a small subset of adenocarcinomas (6%) with worse outcome than other tumors. This subset of tumors exhibited characteristics of intrinsic induction of PD-L1. Importantly, the majority of adenocarcinomas (58%) exhibited prominent CD4/CD8/CD68-positive cells with high or low PD-L1 expression in malignant cells. Investigators recently showed that in melanoma and NSCLC cases, tumors with high PD-L1 expression in malignant cells and high densities of TAICs exhibited durable tumor regression and prolonged disease stabilization when treated with anti-PD-1/PD-L1 drugs (50), representing a group of patients who would benefit from this type of therapy.

In summary, in this study, we showed that multiple factors may be correlated with PD-L1 expression in NSCLC malignant cells and macrophages. We identified different patterns of PD-L1 protein expression and detected the TAIC density in surgically resected adenocarcinoma and SCC specimens. We found that TAIC density varied according to the compartment of the tumor examined and that adenocarcinoma specimens with a solid tumor histology, obtained from smokers, or obtained from patients with airflow limitation had higher expression of immune markers than patients without these characteristics. Also, we identified several immune markers whose expression correlated with outcome of NSCLC; however, future validation of our finding using similar cohort of patients is needed.

Supplementary Material

Refer to Web version on PubMed Central for supplementary material.

Acknowledgments

Grant Support

This study was supported in part by a Department of Defense PROSPECT grant (W81XWH-07-1-0306), the Cancer Prevention Research Institute of Texas Multi-Investigator Research Award (RP120713 and RP150405), the University of Texas Lung Specialized Programs of Research Excellence grant (P50CA70907; to I.I. Wistuba), MD Anderson's Institutional Tissue Bank Award (2P30CA016672) from the National Cancer Institute, R. Lee Clark Fellow (supported by the Jeane F. Shelby Scholarship Fund), Core Grant–NIH Cancer Center Support Grant (CA016672), and National Counsel of Technological and Scientific Development of the Ministry of Science, Technology and Innovation of Brazil (P246042/2012-5).

References

1. Mellman I, Coukos G, Dranoff G. Cancer immunotherapy comes of age. Nature. 2011; 480:480–9. [PubMed: 22193102]
2. Sharpe AH, Wherry EJ, Ahmed R, Freeman GJ. The function of programmed cell death 1 and its ligands in regulating autoimmunity and infection. Nat Immunol. 2007; 8:239–45. [PubMed: 17304234]
3. Sheppard KA, Fitz LJ, Lee JM, Benander C, George JA, Wooters J, et al. PD-1 inhibits T-cell receptor induced phosphorylation of the ZAP70/CD3zeta signalosome anddownstream signaling to PKCtheta. FEBS Lett. 2004; 574:37–41. [PubMed: 15358536]
4. Eggermont AM, Spatz A, Robert C. Cutaneous melanoma. Lancet. 2014; 383:816–27. [PubMed: 24054424]
5. Droeser RA, Hirt C, Viehl CT, Frey DM, Nebiker C, Huber X, et al. Clinical impact of programmed cell death ligand 1 expression in colorectal cancer. Eur J Cancer. 2013; 49:2233–42. [PubMed: 23478000]
6. Ghebeh H, Mohammed S, Al-Omair A, Qattan A, Lehe C, Al-Qudaihi G, et al. The B7-H1 (PD-L1) T lymphocyte-inhibitory molecule is expressed in breast cancer patients with infiltrating ductal carcinoma: correlation with important high-risk prognostic factors. Neoplasia. 2006; 8:190–8. [PubMed: 16611412]
7. Boland JM, Kwon ED, Harrington SM, Wampfler JA, Tang H, Yang P, et al. Tumor B7-H1 and B7-H3 expression in squamous cell carcinoma of the lung. Clin Lung Cancer. 2013; 14:157–63. [PubMed: 22868219]
8. Cooper WA, Tran T, Vilain RE, Madore J, Selinger CI, Kohonen-Corish M, et al. PD-L1 expression is a favorable prognostic factor in early stage non-small cell carcinoma. Lung Cancer. 2015; 89:181–8. [PubMed: 26024796]

9. D'Incecco A, Andreozzi M, Ludovini V, Rossi E, Capodanno A, Landi L, et al. PD-1 and PD-L1 expression in molecularly selected non-small-cell lung cancer patients. Br J Cancer. 2015; 112:95–102. [PubMed: 25349974]
10. Mu CY, Huang JA, Chen Y, Chen C, Zhang XG. High expression of PD-L1 in lung cancer may contribute to poor prognosis and tumor cells immune escape through suppressing tumor infiltrating dendritic cells maturation. Med Oncol. 2011; 28:682–8. [PubMed: 20373055]
11. Velcheti V, Schalper KA, Carvajal DE, Anagnostou VK, Syrigos KN, Sznol M, et al. Programmed death ligand-1 expression in non-small cell lung cancer. Lab Invest. 2014; 94:107–16. [PubMed: 24217091]
12. Romano E, Romero P. The therapeutic promise of disrupting the PD-1/PD-L1 immune checkpoint in cancer: unleashing the CD8 T cell mediated antitumor activity results in significant, unprecedented clinical efficacy in various solid tumors. J Immunother Cancer. 2015; 3:15. [PubMed: 25901287]
13. Anagnostou VK, Brahmer JR. Cancer immunotherapy: a future paradigm shift in the treatment of non-small cell lung cancer. Clin Cancer Res. 2015; 21:976–84. [PubMed: 25733707]
14. Topalian SL, Hodi FS, Brahmer JR, Gettinger SN, Smith DC, McDermott DF, et al. Safety, activity, and immune correlates of anti-PD-1 antibody in cancer. N Engl J Med. 2012; 366:2443–54. [PubMed: 22658127]
15. Kim MY, Koh J, Kim S, Go H, Jeon YK, Chung DH. Clinicopathological analysis of PD-L1 and PD-L2 expression in pulmonary squamous cell carcinoma: comparison with tumor-infiltrating T cells and the status of oncogenic drivers. Lung Cancer. 2015; 88:24–33. [PubMed: 25662388]
16. Gatalica Z, Snyder C, Maney T, Ghazalpour A, Holterman DA, Xiao N, et al. Programmed cell death 1 (PD-1) and its ligand (PD-L1) in common cancers and their correlation with molecular cancer type. Cancer Epidemiol Biomarkers Prev. 2014; 23:2965–70. [PubMed: 25392179]
17. Berghoff AS, Ricken G, Widhalm G, Rajky O, Hainfellner JA, Birner P, et al. PD1 (CD279) and PD-L1 (CD274, B7H1) expression in primary central nervous system lymphomas (PCNSL). Clin Neuropathol. 2014; 33:42–9. [PubMed: 24359606]
18. Zhang Y, Wang L, Li Y, Pan Y, Wang R, Hu H, et al. Protein expression of programmed death 1 ligand 1 and ligand 2 independently predict poor prognosis in surgically resected lung adenocarcinoma. Onco Targets Ther. 2014; 7:567–73. [PubMed: 24748806]
19. Lin C, Chen X, Li M, Liu J, Qi X, Yang W, et al. Programmed death-ligand 1 expression predicts tyrosine kinase inhibitor response and better prognosis in a cohort of patients with epidermal growth factor receptor mutation-positive lung adenocarcinoma. Clin Lung Cancer. 2015; 16:e25–35. [PubMed: 25801750]
20. Edge, SB., Byrd, DR., Compton, CC., Fritz, AG., Greene, FL., Trotti, A. AJCC cancer staging manual. 7. New York, NY: Springer; 2010.
21. Travis, WD., Bambrilla, E., Burke, AP., Marx, A., Nicholson, AG. IARC WHO classification of tumours 2015. 4. Geneva, Switzerland: World Health Organization; 2015. WHO classification of tumours of the lung, pleura, thymus and heart; p. 32-5.
22. Guo C, Shao R, Correa AM, Behrens C, Johnson FM, Raso MG, et al. Prognostic significance of combinations of RNA-dependent protein kinase and EphA2 biomarkers for NSCLC. J Thorac Oncol. 2013; 8:301–8. [PubMed: 23370317]
23. Decramer, M., Vogelmeier, C. Global initiative for chronic obstructive lung disease. 2015. Available from: http://www.goldcopd.it/materiale/2015/GOLD_Report_2015.pdf
24. Teng MW, Ngiow SF, Ribas A, Smyth MJ. Classifying cancers based on T-cell infiltration and PD-L1. Cancer Res. 2015; 75:2139–45. [PubMed: 25977340]
25. Sato M, Larsen JE, Lee W, Sun H, Shames DS, Dalvi MP, et al. Human lung epithelial cells progressed to malignancy through specific oncogenic manipulations. Mol Cancer Res. 2013; 11:638–50. [PubMed: 23449933]
26. Yang CY, Lin MW, Chang YL, Wu CT, Yang PC. Programmed cell death-ligand 1 expression in surgically resected stage I pulmonary adenocarcinoma and its correlation with driver mutations and clinical outcomes. Eur J Cancer. 2014; 50:1361–9. [PubMed: 24548766]

27. Konishi J, Yamazaki K, Azuma M, Kinoshita I, Dosaka-Akita H, Nishimura M. B7-H1 expression on non-small cell lung cancer cells and its relationship with tumor-infiltrating lymphocytes and their PD-1 expression. Clin Cancer Res. 2004; 10:5094–100. [PubMed: 15297412]
28. Loke P, Allison JP. PD-L1 and PD-L2 are differentially regulated by Th1 and Th2 cells. Proc Natl Acad Sci U S A. 2003; 100:5336–41. [PubMed: 12697896]
29. Lee SJ, Jang BC, Lee SW, Yang YI, Suh SI, Park YM, et al. Interferon regulatory factor-1 is prerequisite to the constitutive expression and IFN-gamma-induced upregulation of B7-H1 (CD274). FEBS Lett. 2006; 580:755–62. [PubMed: 16413538]
30. Adams EJ, Green JA, Clark AH, Youngson JH. Comparison of different scoring systems for immunohistochemical staining. J Clin Pathol. 1999; 52:75–7. [PubMed: 10343618]
31. Laurinavicius A, Laurinaviciene A, Dasevicius D, Elie N, Plancoulaine B, Bor C, et al. Digital image analysis in pathology: benefits and obligation. Anal Cell Pathol. 2012; 35:75–8.
32. Fridman WH, Pages F, Sautes-Fridman C, Galon J. The immune contexture in human tumours: impact on clinical outcome. Nat Rev Cancer. 2012; 12:298–306. [PubMed: 22419253]
33. Chen J, Feng Y, Lu L, Wang H, Dai L, Li Y, et al. Interferon-gamma-induced PD-L1 surface expression on human oral squamous carcinoma via PKD2 signal pathway. Immunobiology. 2012; 217:385–93. [PubMed: 22204817]
34. Biswas P, Mantelli B, Sica A, Malnati M, Panzeri C, Saccani A, et al. Expression of CD4 on human peripheral blood neutrophils. Blood. 2003; 101:4452–6. [PubMed: 12531788]
35. Parel Y, Chizzolini C. CD4+ CD8+ double positive (DP) T cells in health and disease. Autoimmun Rev. 2004; 3:215–20. [PubMed: 15110234]
36. Hodge G, Barnawi J, Jurisevic C, Moffat D, Holmes M, Reynolds PN, et al. Lung cancer is associated with decreased expression of perforin, granzyme B and interferon (IFN)-gamma by infiltrating lung tissue T cells, natural killer (NK) T-like and NK cells. Clin Exp Immunol. 2014; 178:79–85. [PubMed: 24894428]
37. Chung KF, Adcock IM. Multifaceted mechanisms in COPD: inflammation, immunity, and tissue repair and destruction. Eur Respir J. 2008; 31:1334–56. [PubMed: 18515558]
38. Arenberg DA, Keane MP, DiGiovine B, Kunkel SL, Strom SR, Burdick MD, et al. Macrophage infiltration in human non-small-cell lung cancer: the role of CC chemokines. Cancer Immunol Immunother. 2000; 49:63–70. [PubMed: 10823415]
39. Chen JJ, Yao PL, Yuan A, Hong TM, Shun CT, Kuo ML, et al. Up-regulation of tumor interleukin-8 expression by infiltrating macrophages: its correlation with tumor angiogenesis and patient survival in non-small cell lung cancer. Clin Cancer Res. 2003; 9:729–37. [PubMed: 12576442]
40. Kuang DM, Zhao Q, Peng C, Xu J, Zhang JP, Wu C, et al. Activated monocytes in peritumoral stroma of hepatocellular carcinoma foster immune privilege and disease progression through PD-L1. J Exp Med. 2009; 206:1327–37. [PubMed: 19451266]
41. Horne ZD, Jack R, Gray ZT, Siegfried JM, Wilson DO, Yousem SA, et al. Increased levels of tumor-infiltrating lymphocytes are associated with improved recurrence-free survival in stage 1A non-small-cell lung cancer. J Surg Res. 2011; 171:1–5. [PubMed: 21571304]
42. Kilic A, Landreneau RJ, Luketich JD, Pennathur A, Schuchert MJ. Density of tumor-infiltrating lymphocytes correlates with disease recurrence and survival in patients with large non-small-cell lung cancer tumors. J Surg Res. 2011; 167:207–10. [PubMed: 19896677]
43. Zhuang X, Xia X, Wang C, Gao F, Shan N, Zhang L, et al. A high number of CD8+ T cells infiltrated in NSCLC tissues is associated with a favorable prognosis. Appl Immunohistochem Mol Morphol. 2010; 18:24–8. [PubMed: 19713832]
44. Mori M, Ohtani H, Naito Y, Sagawa M, Sato M, Fujimura S, et al. Infiltration of CD8+ T cells in non-small cell lung cancer is associated with dedifferentiation of cancer cells, but not with prognosis. Tohoku J Exp Med. 2000; 191:113–8. [PubMed: 10946920]
45. Wakabayashi O, Yamazaki K, Oizumi S, Hommura F, Kinoshita I, Ogura S, et al. CD4+ T cells in cancer stroma, not CD8+ T cells in cancer cell nests, are associated with favorable prognosis in human non-small cell lung cancers. Cancer Sci. 2003; 94:1003–9. [PubMed: 14611679]
46. Takanami I, Takeuchi K, Giga M. The prognostic value of natural killer cell infiltration in resected pulmonary adenocarcinoma. J Thorac Cardiovasc Surg. 2001; 121:1058–63. [PubMed: 11385371]

47. Coca S, Perez-Piqueras J, Martinez D, Colmenarejo A, Saez MA, Vallejo C, et al. The prognostic significance of intratumoral natural killer cells in patients with colorectal carcinoma. Cancer. 1997; 79:2320–8. [PubMed: 9191519]

48. Villegas FR, Coca S, Villarrubia VG, Jimenez R, Chillon MJ, Jareno J, et al. Prognostic significance of tumor infiltrating natural killer cells subset CD57 in patients with squamous cell lung cancer. Lung Cancer. 2002; 35:23–8. [PubMed: 11750709]

49. Domagala-Kulawik J. The role of the immune system in non-small cell lung carcinoma and potential for therapeutic intervention. Transl Lung Cancer Res. 2015; 4:177–90. [PubMed: 25870800]

50. Taube JM, Anders RA, Young GD, Xu H, Sharma R, McMiller TL, et al. Colocalization of inflammatory response with B7-h1 expression in human melanocytic lesions supports an adaptive resistance mechanism of immune escape. Sci Transl Med. 2012; 4:127ra37.

Translational Relevance

Better understanding of PD-L1 expression profile and its interplay with tumor-associated inflammatory cells (TAIC) will provide important insight into the pathogenesis and progression of non–small cell lung carcinoma (NSCLC) and assist in the development of biomarkers for anti-PD-1/PD-L1 therapy or other immunotherapy strategies. We investigated the immunohistochemical PD-L1 expression and TAIC density in a large series of well-characterized NSCLC specimens using image analysis approach. We demonstrated different PD-L1 expression and TAICs density patterns in NSCLC according to tumor histology and differentiation and patients smoking and airflow limitation history. Importantly, we identified four subtypes of tumor microenvironment in this disease and that a subset of tumors exhibiting characteristics of intrinsic induction of PD-L1 had worse outcome.

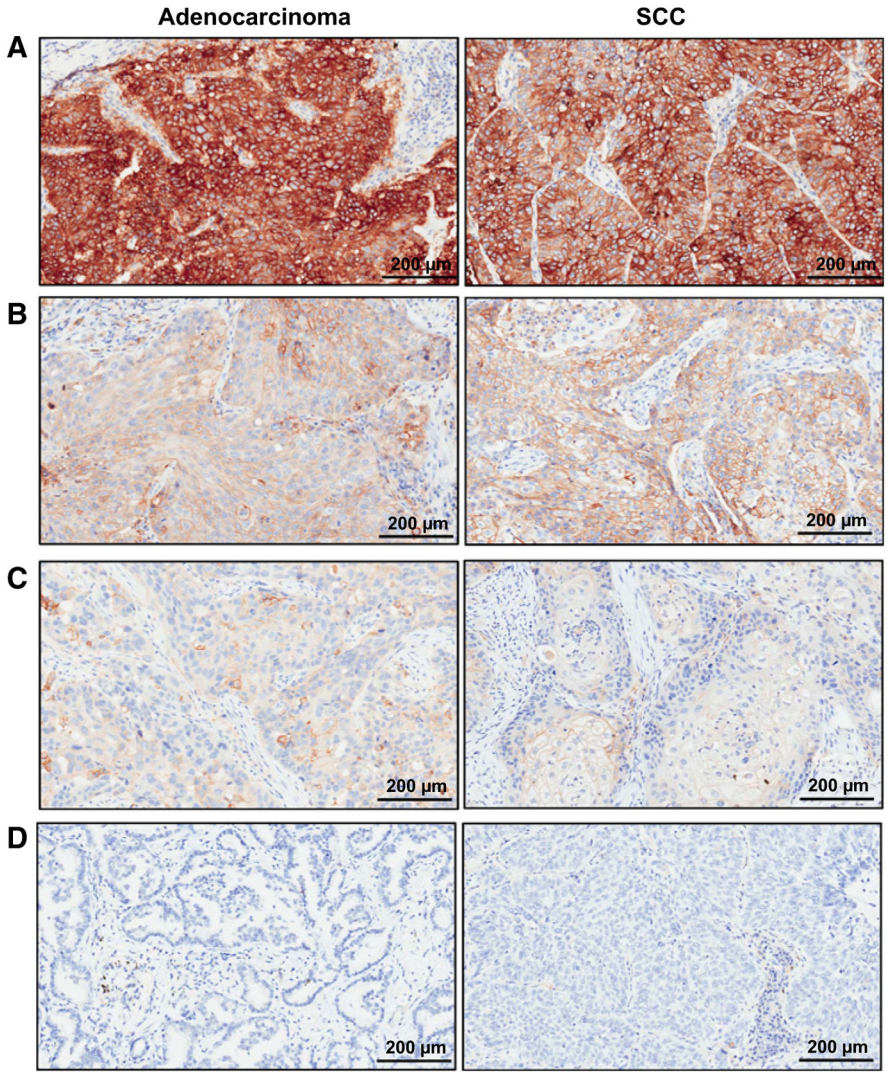

Figure 1.

Microphotographs of representative examples of IHC PD-L1 expression in lung adenocarcinoma and SCC specimens. Four levels of staining (brown) are shown: strong (**A**; staining score, 3+), moderate (**B**; staining score, 2+), weak (**C**; staining score, 1+), and negative (**D**; staining score, 0).

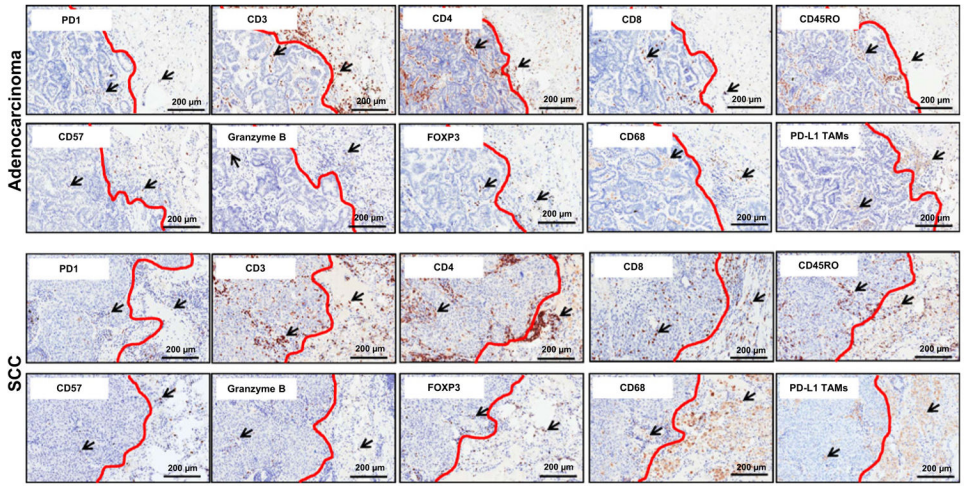

Figure 2.

Microphotographs of representative examples of the 10 immune markers in lung adenocarcinoma and SCC specimens. Red lines divide lung tissue into two compartments: intratumoral (right) and peritumoral (left). Arrows indicate cells expressing each immune marker (brown).

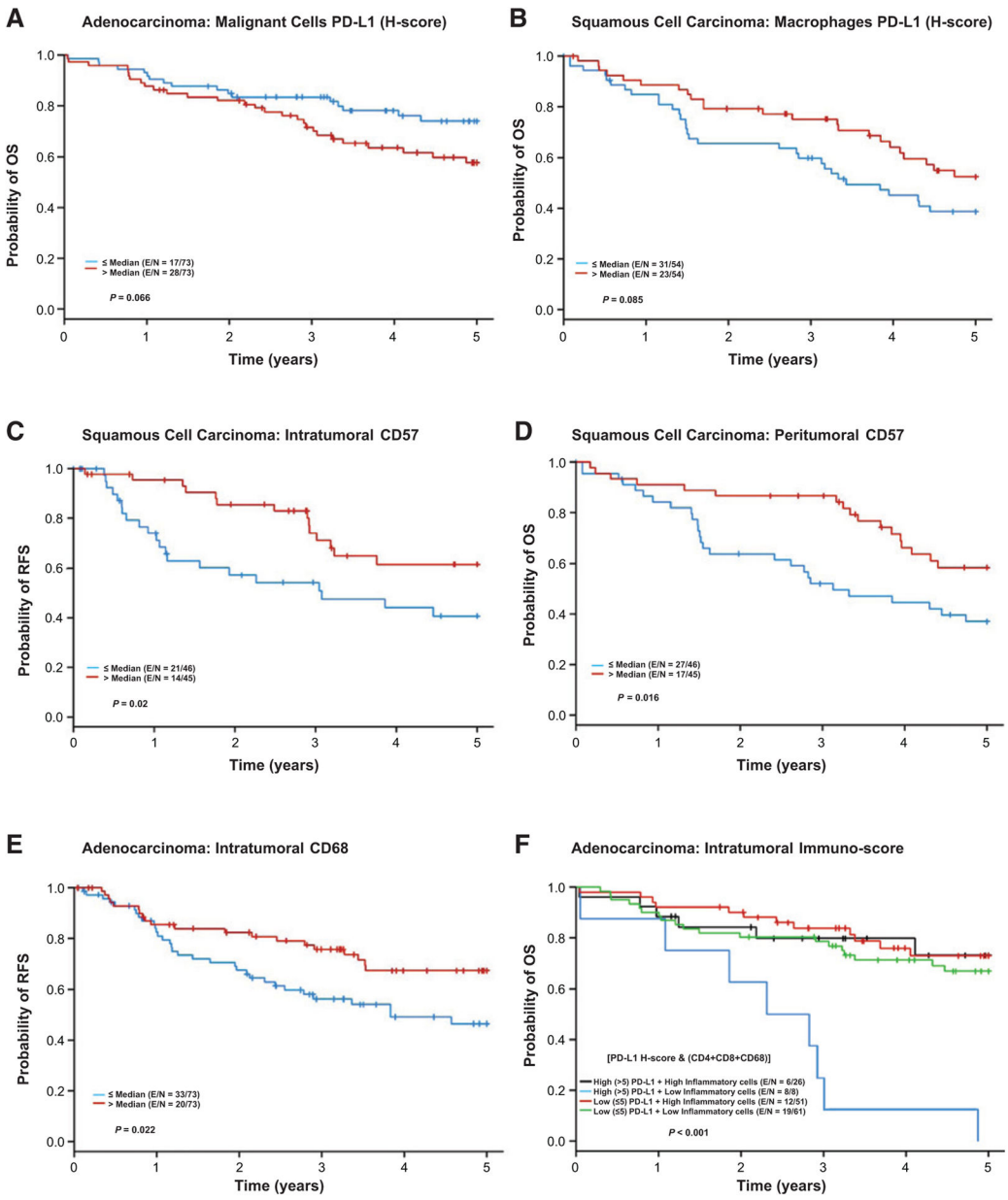

Figure 3.

Kaplan–Meier curves illustrating the prognostic effect on OS and RFS of expression of immune markers in lung adenocarcinoma and SCC specimens.

Table 1

Characteristics of the 254 patients with NSCLC

	n (%)	
Category	**Adenocarcinoma (*n* = 146)**	**SCC (*n* = 108)**
Age		
Median	65.89 y	67.98 y
Sex		
Female	70 (48)	44 (41)
Male	76 (52)	64 (59)
Tobacco history		
No	18 (12)	–
Yes	128 (88)	108 (100)
Smoking status		
Never	18 (12)	–
Former	70 (48)	52 (48)
Current	58 (40)	56 (52)
Tumor size		
Median	3.10 cm	3.85 cm
Tumor status		
T_1	42 (29)	31 (29)
T_2	76 (52)	49 (45)
T_3	21 (14)	24 (22)
T_4	7(5)	4 (4)
Nodal status		
N_0	104 (71)	61 (56)
N_1	24 (16)	32 (30)
N_2	18 (12)	15 (14)
AJCC stage		
I	84 (58)	43 (40)
II	36 (25)	41 (38)
III	26 (18)	24 (22)
Histologic features		
Adenocarcinoma[a]		
Solid	81 (55)	–
Lepidic	20 (14)	–
Acinar	16 (11)	–
Papillary	20 (14)	–
Micropapillary	9(6)	–
SCC		
Well	–	2(2)
Moderate	–	57 (53)

	n (%)	
Category	**Adenocarcinoma (*n* = 146)**	**SCC (*n* = 108)**
Poorly	–	49 (45)
KRAS status[b]		
Mutant	47 (32)	–
Wild-type	97 (66)	–
EGFR status[c]		
Mutant	21 (14)	–
Wild-type	117 (80)	–
Adjuvant therapy		
No	81 (55)	65 (60)
Yes	65 (45)	43 (40)
Vital status at 5 y		
Alive	91 (62)	45 (42)
Dead	55 (38)	63 (58)
Recurrence status at 5 y		
No	89 (61)	62 (57)
Yes	57 (39)	46 (43)

[a] World Health Organization of Lung Cancer.

[b] Mutation status unknown in 2 cases.

[c] Mutation status unknown in 8 cases.

Table 2

Median TAIC density by mm^2 in the intratumoral and peritumoral compartments in lung adenocarcinoma and SCC specimens

	Intratumoral			Peritumoral		
Marker	**Adenocarcinoma**	**SCC**	***P*[a]**	**Adenocarcinoma**	**SCC**	***P*[a]**
CD3	1505.80	1090.00	0.0030	1636.00	2213.70	0.0010
CD4	1217.50	832.00	<0.0001	1425.40	1648.90	0.0700
CD8	866.40	693.20	0.1430	1040.80	1365.60	0.0020
CD57	377.47	208.00	<0.0001	475.40	508.00	0.7600
Granzyme B	236.50	254.10	0.8070	410.60	486.60	0.0490
CD45RO	846.37	913.33	0.1370	1191.80	1725.60	<0.0001
PD-1	521.40	499.63	0.1860	951.80	870.90	0.5810
FOXP3	357.10	335.70	0.6470	435.00	591.80	0.0010
CD68	330.81	201.56	<0.0001	445.54	428.69	0.7740

[a]Kruskal–Wallis test analysis.

Table 3

Distribution of types of microenvironment in NSCLC based on intratumoral malignant cells PD-L1 expression and density of $CD3^+$ TILs

	Intratumoral TILs					
	Adenocarcinoma			SCC		
PD-L1 expression	Negative (%)	Positive (%)	Total	Negative (%)	Positive (%)	Total
Negative	43 (29)	70 (48)	113 (77)	28 (26)	46 (43)	74 (69)
Positive	5(3)	28 (19)	33 (23)	8(7)	26 (24)	34 (31)
Total	48 (33)	98 (67)	146 (100)	36 (33)	72 (67)	108 (100)

NOTE: PD-L1 expression (negative, defined as <5% positive malignant cells membranous expression; positive, >5%) and intratumoral TILs determined by CD3 cells density [negative, defined as mild (lowest tertile) TIL density; positive, defined as moderate and severe density (middle and highest tertiles)].